Maximum Rate Scheduling With Adaptive Modulation in Mixed Impulsive Noise and Additive White Gaussian Noise Environments

Hyungkook Oh, *Member, IEEE*, and Haewoon Nam, *Senior Member, IEEE*

***Abstract*— This article proposes an opportunistic scheduling scheme based on adaptive modulation for users in a mixed noise environment, where some users are under additive white Gaussian noise (AWGN) and other users are exposed to impulsive noise. Unlike the scenario, where all the users are in an AWGN environment, the maximum signal-to-noise ratio (SNR) scheduler does not provide the maximum capacity if users are in a mixed noise environment. In the proposed scheduling scheme, called maximum rate scheduler, the user with the highest rate (or highest modulation order), instead of highest SNR, is selected. To evaluate the performance of the proposed scheduling scheme, the analyses of average spectral efficiency, outage probability and system capacity are provided along with a simple calculation of SNR thresholds for adaptive modulation in an impulsive noise environment satisfying target symbol error rate (SER). Simulation results illustrate that system capacity with the proposed scheduling given target SER $= 10^{-2}$ and the average spectral efficiency are improved by 156% and 124%, respectively, at SNR $= 5$ dB when a strong impulsive noise is present.**

***Index Terms*— Impulsive noise, mixed noise, maximum rate scheduling, multiuser scheduling.**

I. Introduction

AN OPPORTUNISTIC scheduling scheme is often applied in multi-user communication systems to maximize system capacity [1] and is also being considered for future wireless networks [2], [3]. In practical systems, scheduling schemes are commonly used with adaptive modulation to improve average spectral efficiency (ASE) and utilize multi-user diversity among a set of users with different channel qualities.

System capacity and spectral efficiency of a greedy scheduling scheme with adaptive modulation over non-identically independent distributed Nakagami fading channels are analyzed [4]. Also, [5] provides general expressions for the scheduling gains of the opportunistic scheduling with adaptive modulation and its approximations. In [6], [7], performance of multicast system with opportunistic scheduling in the presence of independent and identically distributed (i.i.d.) and non-identically distributed fading channels are analyzed.

Most scheduling schemes are designed to perform optimally in additive white Gaussian noise (AWGN) environment. In some cases, however, communication systems observe Gaussian noise as well as non-Gaussian noise with impulsive characteristics [8]–[12]. Some examples of such an impulsive noise environment are multiple access interference of mobile communication systems with short and burst packets (low duty cycle), radar clutter, and acoustic noise in underwater signal detection [13]. In power line communication (PLC) systems, electromagnetic (EM) noise is caused by switching transients in the power network, where the noise has a short duration with random occurrence and a high-power spectral density [14]. In addition, man-made devices such as microwave ovens and electric motors are impulsive noise sources that often corrupt indoor and outdoor wireless communication systems [15]–[17].

For the optimal systems design, it is important to know the statistics of the instantaneous amplitude of impulsive noise which is an important property for system performance and simulation. The most commonly used impulsive noise is Middle Class A noise model, which is composed of a Rayleigh distribution for the impulsive amplitude and a Poisson distribution for the occurrence of impulses [18]. Middleton noise model fits well to the statistics of the simulated noise by filtering the interference through a PLC channel in a Monte Carlo simulation [19]. In those applications, the impulsive noise severely degrades the performance of communication systems, but a little research outcomes are reported for a scheduling scheme when impulsive noise is present [20], [21].

In wireless mobile communication networks, statistics of impulsive noise are affected by the spatial region of the impulsive noise sources. The spatial region of the impulsive noise sources is commonly assumed to be an infinite plane [22]. However, receivers in many wireless networks may be corrupted by impulsive noise from finite-area regions (e.g., impulsive noise sources localized in space around a cafe) [23], [24]. In case of finite-area regions, impulsive noise affects a very small area in the transmission range of a base station due to propagation characteristics such as pathloss and fading [25]. This is the reason why we assume such an environment, where

Manuscript received May 6, 2019; revised March 9, 2020 and September 13, 2020; accepted December 22, 2020. Date of publication January 12, 2021; date of current version May 10, 2021. This work was supported in part by the National Research and Development Program through the National Research Foundation of Korea (NRF) funded by the Ministry of Science and ICT under Grant 2019M3F6A110610812 and in part by the National Research Foundation of Korea (NRF) grant funded by the Korean Government (MSIT) under Grant 2019R1A2C109009612. The associate editor coordinating the review of this article and approving it for publication was Y. Xin. *(Corresponding author: Haewoon Nam.)*

The authors are with the Division of Electrical Engineering, Hanyang University, Ansan 15588, South Korea (e-mail: haewoon_nam@ieee.org).

Color versions of one or more figures in this article are available at https://doi.org/10.1109/TWC.2021.3049124.

Digital Object Identifier 10.1109/TWC.2021.3049124

some users are under AWGN and other users are exposed to impulsive noise.

In such an environment, where mixed Gaussian noise and impulsive noise are present and some users are under impulsive noise, unlike the scenario with all users in AWGN, the conventional opportunistic scheduling scheme that selects the user with the highest signal-to-noise ratio (SNR) does not always maximize system capacity, since a higher SNR in AWGN does not necessarily guarantee a higher rate than the rate obtained by an even lower SNR in impulsive noise. Thus, when some users are under AWGN and other users are in an impulsive noise environment, an opportunistic scheduling scheme has to find the best user based on the maximum rate, instead of maximum SNR, in both noise environments. To the best of authors' knowledge, an opportunistic scheduling scheme with adaptive modulation for some users in AWGN and others in impulsive noise environments has not been investigated.

Adaptive modulation is commonly used in practical communication systems to improve the spectral efficiency by adapting the transmission rate based on varying channel conditions. For adaptive modulation to work, the whole SNR range is divided into several SNR regions, each of which corresponds to a modulation order, separated by SNR thresholds. The system selects the modulation order that the instantaneous SNR belongs to by switching one modulation to another adaptively when channel condition varies. In an AWGN environment, in general, the SNR thresholds for adaptive modulation can be calculated off-line if the target SER is fixed. In impulsive noise environment, however, the SNR thresholds for adaptive modulation can not be calculated off-line, because the parameters of the impulsive noise model, such as the impulsiveness of the noise environment, need to be estimated first and then the SNR thresholds can be calculated based on those parameters. In addition, the target SER needs to be determined in advance for SNR threshold calculation. Therefore, it is necessary to calculate the SNR thresholds in real-time and on-demand basis in practical systems. Unfortunately, the theoretical SER in impulsive noise environment has infinite exponent terms and multipliers, thus the SNR thresholds are difficult to compute. To resolve the aforementioned problem, a simple calculation method which is very suitable and crucial for practical systems with adaptive modulation in impulsive noise environment.

Motivated by the aforementioned observations, this article proposes an opportunistic scheduling scheme based on the maximum rate for users in mixed noise environment. For the computation of transmission rates in two different noise environments, it is necessary to determine the SNR thresholds for adaptive modulation in both environments. In an impulsive noise environment, however, the exact SNR thresholds are very difficult to obtain, if possible. For applying the proposed scheduling scheme to practical systems, it is worth noting that a simple calculation method of the SNR thresholds is crucial. The main contributions of this article are summarized as follows:

- A maximum rate scheduling scheme is proposed to be used with adaptive modulation in a complex multi-user environment like some users in AWGN and others in an impulsive noise environment.
- A simple and practical calculation method is introduced for SNR thresholds, in adaptive modulation, which satisfy a given target SER for BPSK and M-QAM in an impulsive noise environment.
- Closed form expressions are derived for performance evaluation of average spectral efficiency, outage probability (OP) and system capacity of the proposed scheduling scheme.
- System capacity achieved by the proposed scheduling scheme given the target SER $= 10^{-2}$ and its average spectral efficiency is shown to be improved by 156% and 124% at SNR $= 5$ dB, respectively.

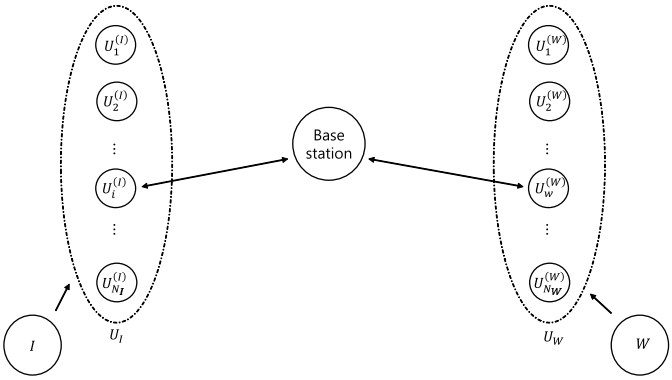

Fig. 1. System model with users in a mixed impulsive noise and AWGN noise. N_I is the number of users in impulsive noise, N_W is the number of users in AWGN, I is an impulsive noise source and W represents AWGN.

This article is organized as follows: Section II introduces noise and system models, while Section III discusses the conventional and proposed scheduling policies. Section IV describes the exact and an approximate symbol error rate of various modulations in impulsive noise. In Section V, simple calculation of SNR thresholds for adaptive modulation in impulsive noise are provided. For performance evaluation, Section VI analyzes average spectral efficiency, outage probability and system capacity of the opportunistic scheduling. Simulation results for performance evaluation of the proposed scheduling are illustrated in Section VII. Finally, this article concludes with a brief summary.

II. System and Noise Models

Consider a base station with a scheduler and a number of users who are under either Gaussian noise or impulsive (non-Gaussian) noise environment, where U_W denotes the set of users in Gaussian noise and U_I is the set of users in impulsive noise, as shown in Fig. 1. Let us assume that there are total $N_W + N_I$ users within the range of the base station, where N_W is the number of users in AWGN environment (N_W is the size of the set U_W) and N_I users are exposed to impulsive noise (N_I is the size of U_I).

For user selection, the base station generally relies on users' channel state information (CSI). Since imperfect CSI may lead to performance degradation, providing the base station an accurate CSI is important for the scheduling scheme although it is difficult in practice [26], [27]. In order to evaluate the

maximum performance of the proposed scheme and compare it with that of the conventional scheme, perfect CSI is firstly assumed. The the accuracy of the performance analysis is verified by simulations. In addition, to show the effect of imperfect CSI on the performance of the proposed scheduling, numerous simulations are performed and the results are shown in Section VII.

When the base station transmits data to a user, the received signal of the jth user is given as

$$x_j = h_j \cdot s + n_j, \tag{1}$$

where h_j is a Rayleigh block fading channel with average power of σ_h^2, s is a transmitted signal with average signal power of σ_s^2, and n_j is a Gaussian noise with average power of σ_W^2 for those users in an AWGN environment or an impulsive noise with average power of σ_I^2 for other users who are under impulsive noise. AWGN and impulsive noise sources are represented by W and I, respectively, in Fig. 1. Note that an impulsive noise and a Gaussian noise are additive white noises having power spectral density of $\frac{\sigma_I^2}{2}$ and $\frac{\sigma_W^2}{2}$, respectively.

For impulsive noise, this article considers Middleton class A noise model, since the Middleton class A model is a good statistical model for electromagnetic interference signals and also agrees well with physical phenomena [28]. The probability density function (PDF) of the instantaneous amplitude of Middleton class A noise is given as

$$f_I(x) = \sum_{m=0}^{\infty} \frac{e^{-A} A^m}{m!} \frac{1}{\sqrt{2\pi\sigma_I^2\sigma_m^2}} e^{-\frac{x^2}{2\sigma_I^2\sigma_m^2}}, \tag{2}$$

where σ_I^2 is average noise power, $\sigma_m^2 = \frac{\frac{m}{A}+\Gamma}{1+\Gamma}$, Γ is defined as the power ratio of Gaussian noise components relative to impulsive noise components, and A is the mean impulsive order. This PDF is a weighted sum of Gaussian distributions with increasing variances, where the weights are determined by Poisson distribution that indicates the probability of appearances of impulsive noise samples. In (2), the term for $m = 0$ is Gaussian noise component and the terms for $m \geq 1$ correspond to non-Gaussian or impulsive noise components, where $m = 1$ is dominant and the contribution of other components with a higher m exponentially decreases as m grows [29]. Unlike the PDF in AWGN, in-phase and quadrature components in Middleton class A noise model are uncorrelated and dependent each other [30].

III. Opportunistic Scheduling Scheme

A. Maximum SNR Scheduling

The opportunistic scheduling scheme, which is also often called as the maximum SNR scheduling scheme, selects the user with the highest SNR at the time of scheduling. In other words, the maximum SNR scheduling scheme assigns the resources to the user with the highest SNR, which guarantees highest data rate under the assumption that all the users are in the same noise, like AWGN, environment. It is known as the scheduling scheme that maximizes overall system capacity or sum rate at the expense of user fairness.

Even though users are in mixed impulsive noise and AWGN environments, the maximum SNR scheduling scheme can still be applied to choose the user with the highest SNR regardless of noise characteristics. The maximum SNR scheduling scheme in such an environment is expressed as

$$u = \arg \max_{w \text{ or } i} \left(\max_{w \in \{U_W\}} \left(\frac{|h_w|^2\sigma_s^2}{\sigma_W^2}\right), \max_{i \in \{U_I\}} \left(\frac{|h_i|^2\sigma_s^2}{\sigma_I^2}\right) \right), \tag{3}$$

where w is the user index for the highest SNR in AWGN, i is the user index for the highest SNR in impulsive noise, and the scheduling algorithm selects the user with the higher SNR between the two.

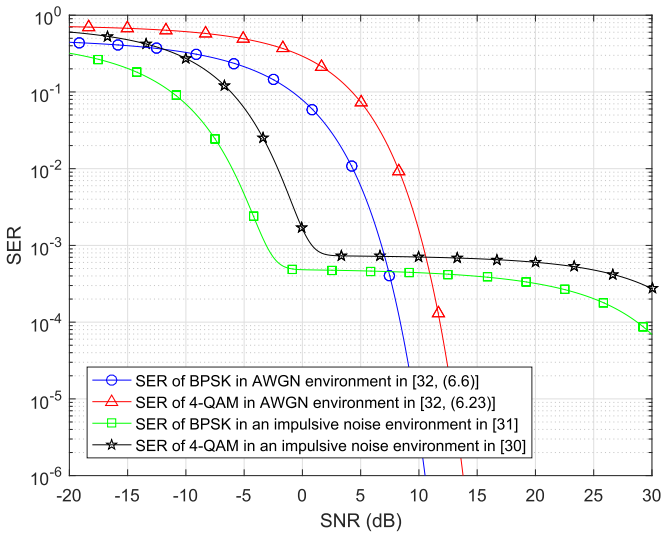

Fig. 2. SERs of BPSK and 4-QAM in an impulsive noise environment with $(A, \Gamma) = (10^{-3}, 0.1)$ and AWGN environment.

Unlike the conventional scenarios of identical noise statistics for all the users, the maximum SNR scheduling scheme does not necessarily maximizes the overall system capacity or sum rate in case of mixed noise environment. This can be understood by the SER performance shown in Fig. 2, which shows the SERs of BPSK and M-QAM in impulsive noise and those in AWGN in [30]–[32]. As shown in the figure, for the SNR of -5 dB, the SER of BPSK in impulsive noise (the line with square markers) is much lower than that in AWGN (circle marker). On the contrary, for the SNR of 10 dB, the SER of BPSK in AWGN is far lower than that in impulsive noise. This fact clearly hints that the maximum SNR scheduling can not provide the maximum performance in mixed noise environments.

B. Maximum Rate Scheduling

As shown in Fig. 2 and mentioned above, the user with the highest SNR does not necessarily provide the minimum SER or the maximum performance when the users are in mixed impulsive noise and AWGN noise environments, because SER performance in impulsive noise is very different from that in AWGN. In order to maximize overall system capacity in mixed noise environments, the proposed scheduling scheme selects the user with the highest transmission rate, instead of highest SNR, where transmission rate is determined for each noise environment separately based on the adaptive modulation (the mapping of transmission rate and SNR) for

each environment. Thus, the scheduling scheme called as the maximum rate scheduling scheme is given by

$$u = \arg \max_{w \text{ or } i} \left(\max_{w \in \{U_W\}} R_W\left(\frac{|h_w|^2 \sigma_s^2}{\sigma_W^2}\right), \max_{i \in \{U_I\}} R_I\left(\frac{|h_i|^2 \sigma_s^2}{\sigma_I^2}\right) \right), \tag{4}$$

where $R_W(\cdot)$ and $R_I(\cdot)$ are transmission rates for a user in AWGN environment and an impulsive noise environment, respectively, and are given in (15).

Note that transmission rate in impulsive noise is totally different from that in AWGN environment because the mapping of an SNR with the corresponding modulation order in impulsive noise is distinctive from that in AWGN environment due to the fact that the SER performance in impulsive noise environment is much different from that in AWGN as already shown in Fig. 2. The details of adaptive modulation in impulsive noise environment including the SNR thresholds used for switching modulations are discussed in Section V.

IV. Symbol Error Rate of BPSK and M-QAM in Impulsive Noise

A. Exact SER Equations

The SER of BPSK in an impulsive noise environment is given as [31]

$$\text{SER} = P_s(T) = e^{-A} \sum_{m=0}^{\infty} \frac{A^m}{m!} Q\left(\sqrt{\frac{2T}{\sigma_m^2}}\right), \tag{5}$$

and the SER of M-QAM in an impulsive noise environment is given as [30]

$$\begin{aligned} \text{SER} &= \frac{(\sqrt{M}-2)^2}{M} \sum_{m=0}^{\infty} \frac{e^{-A}A^m}{m!} \left(4Q\left(\sqrt{\frac{T}{d^2\sigma_m^2}}\right) \right. \\ &\quad \left. - 4Q\left(\sqrt{\frac{T}{d^2\sigma_m^2}}\right)^2 \right) \\ &\quad + \frac{4}{M} \sum_{m=0}^{\infty} \frac{e^{-A}A^m}{m!} \left(2Q\left(\sqrt{\frac{T}{d^2\sigma_m^2}}\right) - Q\left(\sqrt{\frac{T}{d^2\sigma_m^2}}\right)^2 \right) \\ &\quad + \frac{4(\sqrt{M}-2)}{M} \sum_{m=0}^{\infty} \frac{e^{-A}A^m}{m!} \left(3Q\left(\sqrt{\frac{T}{d^2\sigma_m^2}}\right) \right. \\ &\quad \left. - 2Q\left(\sqrt{\frac{T}{d^2\sigma_m^2}}\right)^2 \right), \end{aligned} \tag{6}$$

where $T = \frac{\sigma_s^2}{\sigma_I^2}$ is a received SNR, M is the modulation order, and d^2 equals to 2, 10 and 42 for 4-QAM, 16-QAM and 64-QAM, respectively.

Fig. 2 shows SERs of BPSK and 4-QAM in an impulsive noise environment with $(A, \Gamma) = (10^{-3}, 0.1)$. The SERs of BPSK and 4-QAM in AWGN environment are also plotted for comparison purposes. As can be seen in the figure, the SNR threshold to satisfy the target SER of 10^{-2} in an impulsive noise environment is much smaller than that in AWGN environment. Conversely, the SNR threshold to satisfy the target SER of 10^{-4} in an impulsive noise environment is far larger than that in AWGN environment. This is an interesting fact since a higher modulation order can be adopted for a low SNR condition in impulsive noise environment than what could have been used in AWGN environment while satisfying the given target SER. Thus, user scheduling scheme becomes an intriguing problem when the users are in a mixed AWGN and impulsive noise environment.

B. SER Approximation

In order to achieve higher data rate, current and emerging practical communication systems utilize adaptive modulation, where a modulation order is selected among various modulation orders depending on the received SNR. For adaptive modulation, it is necessary to have the SNR thresholds, by which the user adaptively switches a modulation order to another when the channel condition changes while satisfying the given target SER. Since the SER equations of BPSK and M-QAM in impulsive noise shown in (5) and (6) are too complex, it is very difficult to calculate the exact SNR thresholds of adaptive modulation for impulsive noise. The complexity of the exact SER equations in (5) and (6) comes from the infinite summations. Careful evaluations of the terms in the infinite summation indicate that only a couple of terms are dominant in producing the SER, which is apparently a motivation for an approximation of SER equations [33].

For the SER equation of BPSK in an impulsive noise environment, among the whole m terms in (5), $m = 0$ term is dominant in low SNR regime, whereas $m = 1$ term is dominant in high SNR regime [34]. Thus, using $m \leq 1$ terms, (5) is reduced to

$$\text{SER} \approx \tilde{P}_s(T) = e^{-A} Q\left(\sqrt{\frac{T}{\sigma_0^2}}\right) + e^{-A} A \cdot Q\left(\frac{1}{\sqrt{\alpha}} \sqrt{\frac{T}{\sigma_1^2}}\right). \tag{7}$$

In order to compensate the gap between the true SER given by (5) and the approximate SER by (7) especially in high SNR regime, the SNR ratio α defined as SNR of (5) over SNR of (7) is introduced to reduce the gap. Note that α is close to one when $A < 0.2$, because the infinite m terms are well approximated by two terms ($m \leq 1$) due to sporadic appearances of the noise [35].

Similarly, SER of M-QAM in an impulsive noise environment can be approximated by the dominant terms. Owing to $Q(x)^2 \ll Q(x)$ when x is sufficiently large, (6) can be approximated as

$$\text{SER} \approx e^{-A} P \cdot Q\left(\sqrt{\frac{T}{d^2\sigma_0^2}}\right) + A e^{-A} \cdot P \cdot Q\left(\frac{1}{\sqrt{\alpha}} \sqrt{\frac{T}{d^2\sigma_1^2}}\right), \tag{8}$$

where $P = 2\frac{4}{M} + 3\frac{4(\sqrt{M}-2)}{M} + 4\frac{(\sqrt{M}-2)^2}{M}$. For BPSK, by putting d^2 and P to 1 ($d^2 = P = 1$), (8) is reduced to (7). Note tht P equals to 1, 2, 3 and 7/2 for BPSK, 4-QAM, 16-QAM and 64-QAM, respectively, and d^2 is 1, 2, 10 and 42 for BPSK, 4-QAM, 16-QAM and 64-QAM, respectively.

C. SNR Ratio for SER Approximation

As mentioned earlier, SNR ratio is introduced to compensate the difference between the exact SER and the approximate

TABLE I

SNR RATIO (α) FOR THE TARGET SERS $= 10^{-2}$ AND 10^{-9} IN AN IMPULSIVE NOISE ENVIRONMENT WITH VARIOUS A VALUES

A	0.2	0.3	0.4	0.5
$\alpha_{10^{-2}}$	1.1588	1.2474	1.3428	1.4521
$\alpha_{10^{-9}}$	2.2803	2.5823	2.8445	3.0761
A	0.6	0.7	0.8	0.9
$\alpha_{10^{-2}}$	1.5704	1.6982	1.8365	1.9770
$\alpha_{10^{-9}}$	3.3113	3.5156	3.7325	3.9264

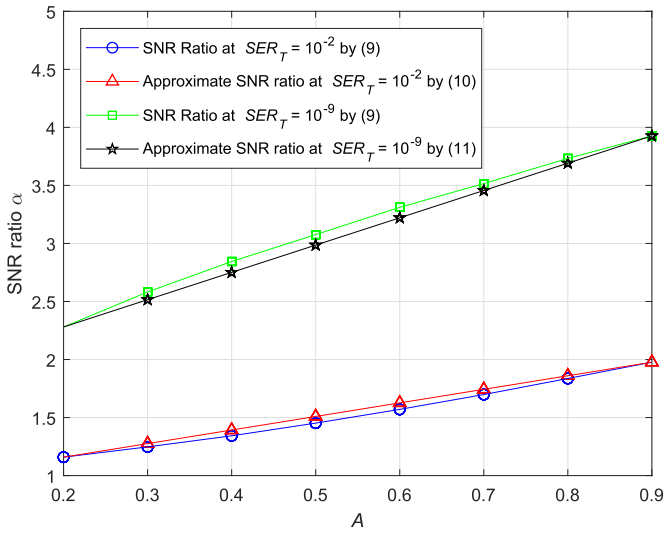

Fig. 3. The exact SNR ratio by (9) and the approximate SNR ratio by (10) and (11) as a function of A in case of impulsive noise with $\Gamma = 10^{-3}$.

SER. For the given target SER SER_T, the SNR ratio is obtained as

$$\alpha = \frac{P_s^{-1}(SER_T)}{\tilde{P}_s^{-1}(SER_T)}, \tag{9}$$

where $P_s(T)$ is the exact SER equation, which is defined in (5) for BPSK, $\tilde{P}_s(T)$ is the approximate SER in (7) for BPSK, and $P_s^{-1}(SER_T)$ and $\tilde{P}_s^{-1}(SER_T)$ are the inverse functions of those SER equations, respectively. The inverse functions $P_s^{-1}(SER_T)$ and $\tilde{P}_s^{-1}(SER_T)$ are used to compute SNR ratio α. Since $P_s^{-1}(SER_T)$ and $\tilde{P}_s^{-1}(SER_T)$ are the function of A and Γ, they are computed off-line. Then, the results are saved in a memory and they are used when they need to compute α.

In the above paragraph, the evaluation for the inverse functions is described. It is correct to compute α by using the generalized equation (9), but its computational complexity is very high. So, for practical systems, we have to propose approximation for α and the approximation will be discussed as follows.

Table I shows the SNR ratio computed by (9) for the target SER $= 10^{-2}$ and 10^{-9}, which are respectively called as $\alpha_{10^{-2}}$ and $\alpha_{10^{-9}}$, in an impulsive noise environment with various A values. In the table, it is noticeable that α is almost linearly proportional to A. Fig. 3 plots the SNR ratio computed by (9) as a function of A when the target SER is 10^{-2} and 10^{-9} to

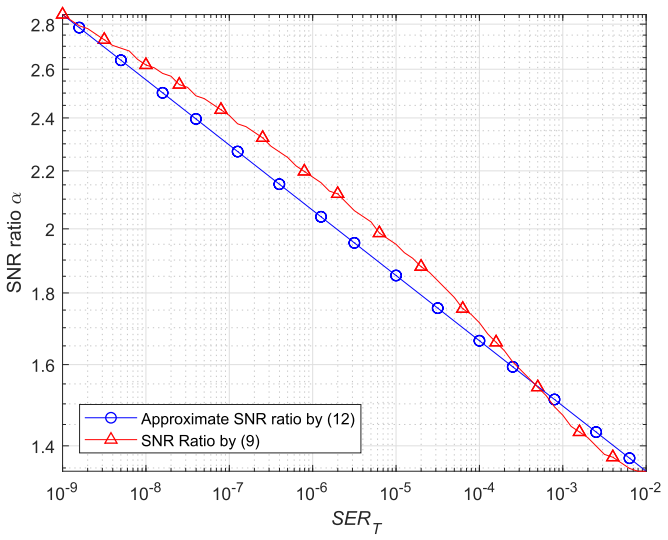

Fig. 4. The exact SNR ratio and the proposed SNR ratio as a function of SER_T in case of impulsive noise with $(A, \Gamma) = (0.4, 10^{-3})$.

confirm that the SNR ratio is almost linearly increasing as A grows. Since SNR ratio is also dependent upon the target SER, further investigations are performed to identify the relationship of SNR ratio with target SER. Fig. 4 shows the relation between SNR ratio and SER in impulsive noise environment with $(A, \Gamma) = (0.4, 10^{-3})$. As shown in the figure, it is clear that SNR ratio is linearly decreasing as target SER increases both in log scale.

Motivated by these observations, a simple formula of calculating SNR ratio as a function of A and a target SER is introduced as follows. Note that the region of interest for a target SER is from 10^{-2} to 10^{-9}. Firstly, α's for the boundary target SERs, 10^{-9} and 10^{-2}, are modeled as linear functions of A. Using the SNR ratios given in Table I, the SNR ratio $\alpha_{10^{-2}}$ is approximated as a linear function of A as

$$\alpha_{10^{-2}} = 1.1689A + 0.9250, \tag{10}$$

and, similarly, the SNR ratio $\alpha_{10^{-9}}$ is presented as a linear function of A as

$$\alpha_{10^{-9}} = 2.3516A + 1.8100. \tag{11}$$

In addition, it is necessary for the computation of SNR ratio to have the relation between SNR ratio and target SER. As shown in Fig. 4, the relation between SNR ratio and target SER in impulsive noise environment is linear when both axes are in log scale. Thus, the SNR ratio can be modeled as a function of A and target SER as

$$\alpha = \begin{cases} c \cdot (SER_T)^k, & \text{for } A \geq 0.2 \\ 1, & \text{for } A < 0.2. \end{cases} \tag{12}$$

where k is the slope of the linear model between SNR ratio and target SER, as shown in Fig. 4, and is computed using $\alpha_{10^{-2}}$ in (10) and $\alpha_{10^{-9}}$ in (11) as

$$k = \frac{\log_{10}(\alpha_{10^{-2}}) - \log_{10}(\alpha_{10^{-9}})}{\log_{10}(10^{-2}) - \log_{10}(10^{-9})} = \frac{1}{7}\log_{10}\left(\frac{1.1689A + 0.9250}{2.3516A + 1.81}\right), \tag{13}$$

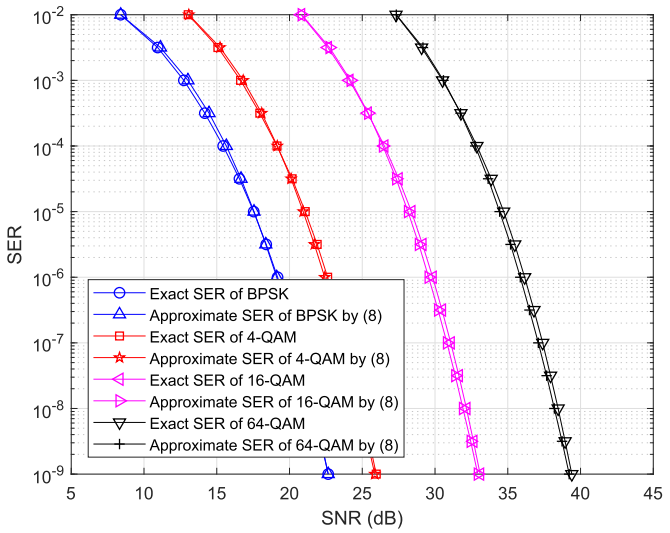

Fig. 5. Comparison between approximate SER in (8) and exact SER of BPSK and M-QAM in $(A, \Gamma) = (0.2, 10^{-3})$.

and c is computed by setting $SER_T = 10^{-2}$ in (12) as

$$c = \alpha_{10^{-2}} 100^k = \frac{(1.1689A + 0.9250)^{\frac{9}{7}}}{(2.3516A + 1.81)^{\frac{2}{7}}}. \tag{14}$$

As mentioned earlier, α can be ignored when $A < 0.2$ since the infinite m terms in the impulsive noise model are well approximated by two terms ($m \leq 1$) due to sporadic appearances of the noise [35]. Fig. 5 illustrates comparison between the approximate and the exact SERs of BPSK and M-QAM in $(A, \Gamma) = (0.2, 10^{-3})$. As shown in Fig. 5, the SNR gap between the exact and the approximate SERs of BPSK and M-QAM are is indistinguishable due to the compensation by SNR ratio in the approximate SERs.

V. Adaptive Modulation and the SNR Thresholds in Impulsive Noise

Adaptive modulation is one of the most effective techniques to maximize the transmission rate by taking advantage of channel fading while maintaining the required error performance such as SER. The key parameter in adaptive modulation is the SNR thresholds, by which a user adaptively switches a modulation order to another when the channel condition changes while satisfying the given target SER. This section describes how to calculate the SNR thresholds for adaptive modulation in AWGN and an impulsive noise environments.

A. Transmission Rates in Adaptive Modulation

Suppose that BPSK and M-QAM, where $M = 4$, 16, and 64, are used for the adaptive modulation, where the whole SNR range is partitioned into five non-overlapping consecutive intervals. When the user's instantaneous SNR falls into one of the partitioned SNR ranges, the base station allows the user to transmit data at the corresponding modulation order. Thus, the transmission rate $R(x)$ is given as

$$R(x) = \begin{cases} 0, & 0 \leq x < \gamma_{[2]}, \text{ no transmission} \\ 1, & \gamma_{[M]} \leq x < \gamma_{[2M]}, \text{ for BPSK } (M=2) \\ \log_2(M), & \gamma_{[M]} \leq x < \gamma_{[4M]}, \ M = 4, 16, \text{ or } 64, \end{cases} \tag{15}$$

where $\gamma_{[M]}$ is the SNR threshold for switching to BPSK if $M = 2$ or M-QAM if $M = 4$, 16, or 64, while satisfying the target SER. Assume that the upper threshold for the highest modulation order is infinity ($\gamma_{[256]} = \infty$). Note that the lowest SNR range does not allow the user to transmit since the received SNR is not high enough to guarantee the given target SNR. The transmission rate for AWGN is defined based on (15), $R_W(x) = R(x)$, when the SNR thresholds for AWGN given in Section V-B are used. Similarly, the transmission rate for impulsive noise is characterized, $R_I(x) = R(x)$, by the SNR thresholds for impulsive noise instead. The SNR thresholds for impulsive noise are computed in Section V-C.

B. SNR Thresholds for Adaptive Modulation in AWGN

Based on the exact closed form for SER of BPSK in AWGN environment [32, (6.6)], the SNR threshold $\gamma_{[2]}$ is obtained as

$$\gamma_{[2]} = \frac{1}{2}\left(Q^{-1}(\text{SER})\right)^2, \tag{16}$$

where $Q^{-1}(\cdot)$ is the inverse Q function. Furthermore, the exact closed form for SER of M-QAM ($M = 4, 16, 64$) in AWGN environment [32, (6.23)] leads to the SNR threshold $\gamma_{[M]}$ given as

$$\gamma_{[M]} = \frac{M-1}{3}\left(Q^{-1}\left(\frac{\sqrt{M}(1-\sqrt{1-\text{SER}})}{2(\sqrt{M}-1)}\right)\right)^2. \tag{17}$$

In short, the SNR thresholds γ_M for BPSK and M-QAM in AWGN environment are computed as

$$\gamma_{[M]} = \begin{cases} \frac{1}{2}\left(Q^{-1}(\text{SER})\right)^2, \\ \quad \text{for BPSK} \\ \frac{M-1}{3}\left(Q^{-1}\left(\frac{\sqrt{M}(1-\sqrt{1-\text{SER}})}{2(\sqrt{M}-1)}\right)\right)^2, \\ \quad \text{for } M\text{-QAM}. \end{cases} \tag{18}$$

C. SNR Thresholds for Adaptive Modulation in Impulsive Noise

Since the exact SER equations of BPSK and M-QAM for impulsive noise shown in (5) and (6) are too complex, the SNR thresholds for BPSK and M-QAM are calculated based on the SER approximation given in (8). Before computing SNR thresholds of BPSK and M-QAM in an impulsive noise environment using the approximate SER, some analysis of (8) is performed regarding the relation between target SER and A. The analysis reveals that e^{-A} term is sufficiently dominant in (8) when target SER is larger than A, and otherwise Ae^{-A} term is dominant. Based on this analysis, the SER equation

TABLE II
SNR THRESHOLDS FOR BPSK, 4-QAM, 16-QAM AND 64-QAM WITH THE TARGET SER $= 10^{-2}$ IN AN IMPULSIVE NOISE ENVIRONMENT WITH $(A, \Gamma) = (10^{-3}, 0.1)$ AND $(A, \Gamma) = (0.2, 10^{-3})$

	BPSK	4-QAM	16-QAM	64-QAM
SNR threshold (dB) in (22) in an impulsive noise environment with $(A, \Gamma) = (10^{-3}, 0.1)$	-6.09	-2.20	5.24	11.64
SNR threshold (dB) in (22) in an impulsive noise environment with $(A, \Gamma) = (0.2, 10^{-3})$	7.76	12.44	20.20	26.69
SNR threshold (dB) in (18) in AWGN environment	4.32	8.22	15.66	22.05

of BPSK and M-QAM to satisfy target SER can be even simplified as

$$\text{SER} \approx \begin{cases} e^{-A} \cdot P \cdot Q\left(\sqrt{\dfrac{T}{d^2\sigma_0^2}}\right), & \text{for } A \leq \text{SER} \\ Ae^{-A} \cdot P \cdot Q\left(\dfrac{1}{\sqrt{\alpha}}\sqrt{\dfrac{T}{d^2\sigma_1^2}}\right), & \text{for } A > \text{SER}. \end{cases} \tag{19}$$

Therefore, in the case of $A \leq$ SER, the SNR threshold $\gamma_{[M]}$ is computed as

$$\gamma_{[M]} = d^2\sigma_0^2 \left(Q^{-1}\left(\frac{\text{SER}}{e^{-A}P}\right)\right)^2, \tag{20}$$

and, in the case of $A >$ SER, the SNR threshold $\gamma_{[M]}$ becomes

$$\gamma_{[M]} = \alpha d^2\sigma_1^2 \left(Q^{-1}\left(\frac{\text{SER}}{Pe^{-A}A}\right)\right)^2. \tag{21}$$

Finally, putting (20) and (21) together, the SNR threshold $\gamma_{[M]}$ for BPSK and M-QAM for adaptive modulation in impulsive noise is simply determined as

$$\gamma_{[M]} = \begin{cases} d^2\sigma_0^2 \left(Q^{-1}\left(\frac{\text{SER}}{e^{-A}P}\right)\right)^2, & \text{for } A \leq \text{SER} \\ \alpha d^2\sigma_1^2 \left(Q^{-1}\left(\frac{\text{SER}}{Pe^{-A}A}\right)\right)^2, & \text{for } A > \text{SER}. \end{cases} \tag{22}$$

Table II shows the SNR thresholds for adaptive modulation in AWGN environment and those in impulsive noise environment with various noise parameters $(A, \Gamma) = (10^{-3}, 0.1)$ and $(A, \Gamma) = (0.2, 10^{-3})$ when target SER is 10^{-2}. In the case of the noise parameter of $(A, \Gamma) = (10^{-3}, 0.1)$, where the target SER is larger than A ($A \leq$ SER), the difference of SNR thresholds for AWGN and an impulsive noise is about 10.41 dB, i.e. σ_0^2, because SNR threshold for an impulsive noise strongly depends on σ_0^2. On the other hand, in the case of $(A, \Gamma) = (0.2, 10^{-3})$, where the target SER is smaller than A ($A >$ SER), SNR threshold for an impulsive noise is larger than that for AWGN, because the SNR threshold depends on σ_1^2.

VI. PERFORMANCE ANALYSIS OF SCHEDULING POLICIES

This section analyzes performance of the proposed maximum rate scheduling scheme using adaptive modulation in impulsive noise. For comparison purposes, the performance of the conventional maximum SNR scheduling scheme in AWGN environment is also shown. In Section VI-A, the PDF and cumulative density function (CDF) expressions of received SNR based on the maximum SNR and maximum rate scheduling schemes are derived. In Section VI-B, closed forms of average spectral efficiency of the two scheduling scheme are discussed. In addition, outage probabilities of the two scheduling schemes are computed in Section VI-C, followed by capacity expressions of the two scheduling schemes.

A. CDF and PDF of Received SNR for the Scheduling Schemes

To evaluate the performance of the proposed maximum rate scheduling scheme and compare it with that of the conventional maximum SNR scheduling scheme, it is necessary to analyze the CDF and the PDF of the received SNR of both scheduling schemes as follows.

Firstly, since the maximum SNR scheduling in (3) selects the user with highest received SNR, the CDF of the received SNR based on the maximum SNR scheduling scheme is calculated as

$$F_c(x) = \Big(\int_0^x \lambda_W e^{-\lambda_W t} dt\Big)^{N_W+N_I} = (1-e^{-\lambda_W x})^{N_W+N_I}, \tag{23}$$

where $\lambda_W = \frac{\sigma_W^2}{\sigma_s^2\sigma_h^2}$, and N_W and N_I are the number of users in AWGN and impulsive noise environments, respectively. By differentiating (23), the PDF of the received SNR based on the maximum SNR scheduling scheme is obtained as

$$f_c(x) = (N_W+N_I)(1-e^{-\lambda_W x})^{N_W+N_I-1}\lambda_W e^{-\lambda_W x}. \tag{24}$$

Meanwhile, since the maximum rate scheduling first selects the users with the highest data rate in impulsive noise and AWGN environments, the CDF is computed by multiplying the CDF of the highest received SNR in AWGN and that of the highest in impulsive noise environment. Thus, the CDF for the maximum rate scheduling scheme is given by

$$F_p(x) = F_I(x)F_W(x), \tag{25}$$

where $F_W(x)$ and $F_I(x)$ are CDFs of the received SNR of users with highest SNR in AWGN and impulsive noise environments, respectively. Since $F_W(x)$ is the CDF of received

SNR of a user with highest received SNR in AWGN environment, $F_W(x)$ is computed as

$$F_W(x) = \Big(\int_0^x \lambda_W e^{-\lambda_W t} dt \Big)^{N_W} = \big(1 - e^{-\lambda_W x}\big)^{N_W}, \quad (26)$$

whereas $F_I(x)$ is given as

$$F_I(x) = \Big(\int_0^x \lambda_I e^{-\lambda_I t} dt \Big)^{N_I} = \big(1 - e^{-\lambda_I x}\big)^{N_I}, \quad (27)$$

where λ_I equals to

$$\lambda_I = \begin{cases} \dfrac{\sigma_I^2 \sigma_0^2}{\sigma_s^2 \sigma_h^2}, & \text{for } SER_T \geq A \\ \dfrac{\sigma_I^2 \alpha \sigma_1^2}{\sigma_s^2 \sigma_h^2}, & \text{for } SER_T < A. \end{cases} \quad (28)$$

Finally, by substituting (26) and (27) into (25), the CDF of received SNR for the maximum rate scheduling scheme is obtained as

$$F_p(x) = \big(1 - e^{-\lambda_I x}\big)^{N_I} \big(1 - e^{-\lambda_W x}\big)^{N_W}. \quad (29)$$

By differentiating (29), the PDF of received SNR based on the maximum rate scheduling scheme is derived as

$$\begin{aligned} & f_p(x) \\ &= N_I \big(1 - e^{-\lambda_I x}\big)^{N_I - 1} \lambda_I e^{-\lambda_I x} \big(1 - e^{-\lambda_W x}\big)^{N_W} \\ &\quad + \big(1 - e^{-\lambda_I x}\big)^{N_I} N_W \lambda_W e^{-\lambda_W x} \big(1 - e^{-\lambda_W x}\big)^{N_W - 1}. \end{aligned} \quad (30)$$

B. Average Spectral Efficiency

Based on the probability distributions of received SNR for the two scheduling schemes above, the average spectral efficiency of scheduling schemes with adaptive modulation is given as [36]

$$\text{ASE} = \int_{\gamma_{[2]}}^{\gamma_{[4]}} f(x) dx + \sum_{n \in \{4,16,64\}} \log_2(n) \int_{\gamma_{[n]}}^{\gamma_{[4n]}} f(x) dx, \quad (31)$$

where $f(x)$ is the distribution of the received SNR based on a scheduling scheme, and $\gamma_{[M]}$ represents the SNR threshold for BPSK or M-QAM.

By inserting (18) and (24) into (31), the average spectral efficiency of the maximum SNR scheduling scheme is given by

$$\begin{aligned} & \text{ASE}_{(c)} \\ &= 6 - 2\big(1 - e^{-\lambda_W \gamma_{64}^{(w)}}\big)^{N_W + N_I} \\ &\quad - 2\big(1 - e^{-\lambda_W \gamma_{16}^{(w)}}\big)^{N_W + N_I} - \big(1 - e^{-\lambda_W \gamma_4^{(w)}}\big)^{N_W + N_I} \\ &\quad - \big(1 - e^{-\lambda_W \gamma_2^{(w)}}\big)^{N_W + N_I}. \end{aligned} \quad (32)$$

Likewise, by substituting (22) and $f_p(x)$ in (30) into (31), the average spectral efficiency of the maximum rate scheduling scheme is obtained as

$$\begin{aligned} \text{ASE}_{(p)} &= 6 - 2\big(1 - e^{-\lambda_I \gamma_{64}^{(w)}}\big)^{N_I} \big(1 - e^{-\lambda_W \gamma_{64}^{(w)}}\big)^{N_W} \\ &\quad - 2\big(1 - e^{-\lambda_I \gamma_{16}^{(w)}}\big)^{N_I} \big(1 - e^{-\lambda_W \gamma_{16}^{(w)}}\big)^{N_W} \\ &\quad - \big(1 - e^{-\lambda_I \gamma_4^{(w)}}\big)^{N_I} \big(1 - e^{-\lambda_W \gamma_4^{(w)}}\big)^{N_W} \\ &\quad - \big(1 - e^{-\lambda_I \gamma_2^{(w)}}\big)^{N_I} \big(1 - e^{-\lambda_W \gamma_2^{(w)}}\big)^{N_W}. \end{aligned} \quad (33)$$

C. Outage Probability

Outage probability is an important performance metric for a scheduling scheme to evaluate the availability of the services provided by the system. Due to no transmission under the lowest SNR threshold in adaptive modulation, outage probability is simply computed as

$$P_{out} = F(\gamma_{[2]}), \quad (34)$$

where the $F(x)$ is the CDF of a scheduling scheme evaluated at x.

For the maximum SNR scheduling scheme, substituting (23) into (34) gives the outage probability as

$$\begin{aligned} P_{out}^{(c)} &= \Big(\int_0^{\gamma_{[2]}} \lambda_W e^{-\lambda_W t} dt \Big)^{N_W + N_I} \\ &= \big(1 - e^{-\lambda_W \gamma_{[2]}}\big)^{N_W + N_I}. \end{aligned} \quad (35)$$

Similarly, substituting (25) into (34), the outage probability of the maximum rate scheduling scheme is obtained by

$$\begin{aligned} P_{out}^{(p)} &= \Big(\int_0^{\gamma_2^{(w)}} \lambda_I e^{-\lambda_I t} dt \Big)^{N_I} \Big(\int_0^{\gamma_2^{(w)}} \lambda_W e^{-\lambda_W t} dt \Big)^{N_W} \\ &= \big(1 - e^{-\lambda_I \gamma_2^{(w)}}\big)^{N_I} \big(1 - e^{-\lambda_W \gamma_2^{(w)}}\big)^{N_W}. \end{aligned} \quad (36)$$

D. System Capacity

System capacity is defined as the maximum data rate that a wireless communication system can achieve and is the most crucial performance metric for a scheduling scheme.

Given an average transmit power constraint, system capacity with rate adaptation is given by [37]

$$C = \int_{\gamma_{[2]}}^{\infty} \log_2 \left(\frac{x}{\gamma_{[2]}} \right) f(x) dx. \quad (37)$$

Firstly, the system capacity of the maximum SNR scheduling scheme is computed based on the PDF of the received SNR in (24). For computation of system capacity, (24) is rewritten by the binomial expansion as

$$\begin{aligned} f_c(x) &= (N_W + N_I) \lambda_W \\ &\quad \times \sum_{k=0}^{N_W + N_I - 1} (-1)^k \binom{N_I + N_W - 1}{k} e^{-(1+k)\lambda_W x}, \end{aligned} \quad (38)$$

where $\binom{N}{K}$ denotes the binomial coefficient given by

$$\binom{N}{K} = \frac{(N)!}{(N-K)!K!}. \quad (39)$$

Then, inserting (38) into $f(x)$ in (37) provides the system capacity of the maximum SNR scheduling scheme as

$$\begin{aligned} C^{(c)} &= \int_{\gamma_2^{(w)}}^{\infty} \log_2\left(\frac{x}{\gamma_2^{(w)}}\right)(N_W+N_I)\lambda_W \\ &\quad \times \sum_{k=0}^{N_W+N_I-1} (-1)^k \binom{N_I+N_W-1}{k} e^{-(1+k)\lambda_W x} dx \\ &= (N_W+N_I)\log_2(e) \\ &\quad \times \sum_{k=0}^{N_W+N_I-1} (-1)^k \binom{N_W+N_I-1}{k} \\ &\quad \times \frac{E_1\left((1+k)\gamma_2^{(w)}\lambda_W\right)}{1+k}, \end{aligned} \tag{40}$$

where, when $x \geq 0$, $E_1(x)$ is the exponential integral of first-order function defined as

$$E_1(x) = \int_1^{\infty} \frac{e^{-xt}}{t} dt. \tag{41}$$

Similarly, using the PDF of the received SNR in (30), the system capacity for the maximum rate scheduling scheme is obtained as follows. By the binomial expansion, (30) is rewritten as

$$\begin{aligned} f_p(x) = \sum_{k=0}^{N_I-1} \binom{N_I-1}{k} \sum_{l=0}^{N_W-1} \binom{N_W-1}{l} \\ \times (-1)^{k+l}(f_1(x)+f_2(x)-f_3(x)), \end{aligned} \tag{42}$$

where

$$\begin{aligned} f_1(x) &= N_I\lambda_I e^{-((k+1)\lambda_I+l\lambda_W)x}, \\ f_2(x) &= N_W\lambda_W e^{-(k\lambda_I+(l+1)\lambda_W)x}, \\ f_3(x) &= (N_W\lambda_W+N_I\lambda_I)e^{-((k+1)\lambda_I+(l+1)\lambda_I)x}. \end{aligned} \tag{43}$$

Inserting $f_1(x)$ into $f(x)$ in (37), the system capacity by the first term is given as

$$\begin{aligned} C_1 &= \int_{\gamma_2^{(w)}}^{\infty} \log_2\left(\frac{x}{\gamma_2^{(w)}}\right) N_I\lambda_I e^{-((k+1)\lambda_I+l\lambda_W)x} dx \\ &= \int_1^{\infty} N_I\lambda_I\gamma_2^{(w)} \log_2(t) e^{-((k+1)\lambda_I+l\lambda_W)\gamma_2^{(w)}t} dt \\ &= \frac{\log_2(e)N_I\lambda_I}{(k+1)\lambda_I+l\lambda_W} \int_1^{\infty} \frac{1}{t} e^{-((k+1)\lambda_I+l\lambda_W)\gamma_2^{(w)}t} dt \\ &= N_I\lambda_I \log_2(e) \frac{E_1\left(((k+1)\lambda_I+l\lambda_W)\gamma_2^{(w)}\right)}{(k+1)\lambda_I+l\lambda_W}. \end{aligned} \tag{44}$$

Subsequently, substituting $f_2(x)$ and $f_3(x)$ into $f(x)$ in (37), the system capacities by the second and the third terms are obtained as

$$\begin{aligned} C_2 &= \int_{\gamma_2^{(w)}}^{\infty} \log_2\left(\frac{x}{\gamma_2^{(w)}}\right) N_W\lambda_W e^{-(k\lambda_I+(l+1)\lambda_W)x} dx \\ &= \int_1^{\infty} N_W\lambda_W\gamma_2^{(w)} \log_2(t) e^{-(k\lambda_I+(l+1)\lambda_W)\gamma_2^{(w)}t} dt \\ &= \frac{\log_2(e)N_W\lambda_W}{k\lambda_I+(l+1)\lambda_W} \int_1^{\infty} e^{-(k\lambda_I+(l+1)\lambda_W)\gamma_2^{(w)}t} dt \\ &= N_W\lambda_W \log_2(e) \frac{E_1\left((k\lambda_I+(l+1)\lambda_W)\gamma_2^{(w)}\right)}{k\lambda_I+(l+1)\lambda_W}, \end{aligned} \tag{45}$$

and

$$\begin{aligned} C_3 &= \int_{\gamma_2^{(w)}}^{\infty} \log_2\left(\frac{x}{\gamma_2^{(w)}}\right)(N_W\lambda_W+N_I\lambda_I) \\ &\quad \times e^{-((k+1)\lambda_I+(l+1)\lambda_I)x} dx \\ &= \int_1^{\infty} (N_W\lambda_W+N_I\lambda_I)\gamma_2^{(w)} \\ &\quad \times \log_2(t) e^{-((k+1)\lambda_I+(l+1)\lambda_W)\gamma_2^{(w)}t} dt \\ &= \frac{\log_2(e)(N_W\lambda_W+N_I\lambda_I)}{(k+1)\lambda_I+(l+1)\lambda_w} \\ &\quad \times \int_1^{\infty} \frac{1}{t} e^{-((k+1)\lambda_I+(l+1)\lambda_W)\gamma_2^{(w)}} dt \\ &= (N_W\lambda_W+N_I\lambda_I)\log_2(e) \\ &\quad \times \frac{E_1\left(((k+1)\lambda_I+(l+1)\lambda_W)\gamma_2^{(w)}\right)}{(k+1)\lambda_I+(l+1)\lambda_W}. \end{aligned} \tag{46}$$

Finally, putting all the pieces in (44), (45) and (46) together, the system capacity for the maximum rate scheduling scheme is presented as (47) as shown at the bottom of the next page.

VII. Simulation Results

For simulations, it is assumed that there are a base station and $N_I + N_W$ users, where $N_I = N_W = 10$. The channel between the base station and the users is Rayleigh block faded with the average power of σ_h^2, where the average power of AWGN and that of impulsive noise are identical and normalized. Complex impulsive noise samples are generated based on the noise model in (2), while the real and the imaginary components are dependent and uncorrelated. In order to evaluate channel estimation error on the performance of the proposed scheduling scheme, scenarios with perfect CSI and imperfect CSI are considered. For the scenario with imperfect CSI, mathematical analysis of the performance is very challenging and intractable, thus we performed numerous simulations to evaluate the performance. To consider imperfect CSI, the estimated channel is modeled as

$$\hat{h} = h + h_e, \tag{48}$$

where $h \sim \mathcal{CN}(0, \sigma_h^2)$ is the true channel gain and $h_e \sim \mathcal{CN}(0, \sigma_{h_e}^2)$ is the channel estimate error that is independent of h and is complex Gaussian distributed with the power of σ_e^2. In addition, the ratio of the variance of channel estimation error relative to signal energy is assumed to be a constant, that is

$$\frac{\sigma_s^2}{\sigma_e^2} = 10^{-2}, \tag{49}$$

where σ_s^2 is the signal energy and σ_e^2 is the variance of channel estimation error.

Fig. 6 shows the SERs of adaptive modulation with the SNR thresholds $\gamma_{[M]}$ in (18) when the target SER is 10^{-2}. The figure shows multiple SNR thresholds demarcated by the SNR thresholds and the modulation order is switched to higher ones as the SNR increases.

Fig. 7 illustrates SERs of adaptive modulation with the proposed SNR threshold $\gamma_{[M]}$ in (22) in an impulsive noise environment with the noise parameter of $(A, \Gamma) = (10^{-3}, 0.1)$,

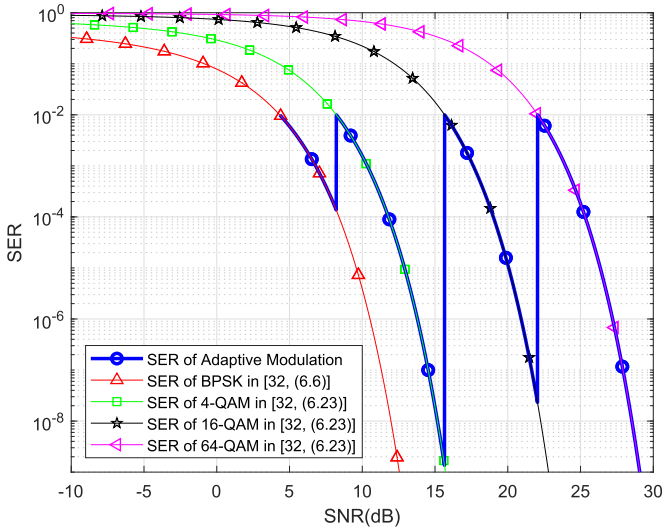

Fig. 6. SERs of adaptive modulation with the SNR threshold $\gamma_{[M]}$ in (18), theoretical BPSK, QPSK, 16-QAM and 64-QAM in AWGN environment.

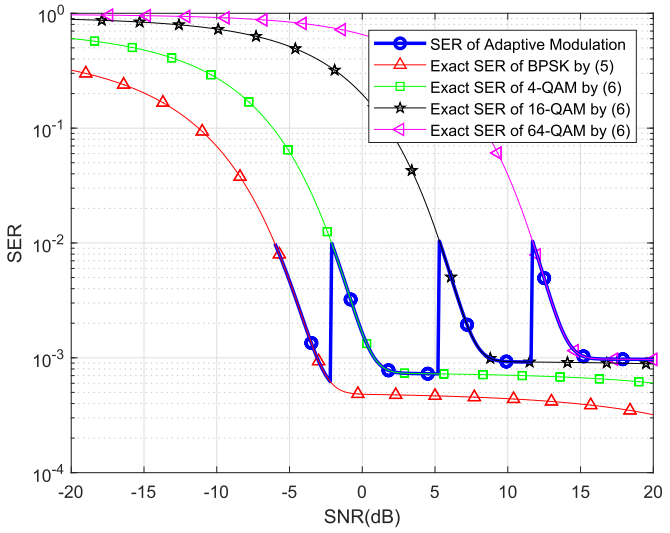

Fig. 7. SERs of adaptive modulation with the proposed SNR threshold $\gamma_{[M]}$ in (22), theoretical BPSK, QPSK, 16-QAM and 64-QAM systems in $(A, \Gamma) = (10^{-3}, 0.1)$.

which has a strong impulsiveness. The target SNR of 10^{-2} is considered. Compared to the SNR thresholds for adaptive modulation in AWGN shown in Fig. 6, the SNR thresholds for adaptive modulation in impulsive noise environment given by (22) are much lower and show a potential of achieving a higher throughput.

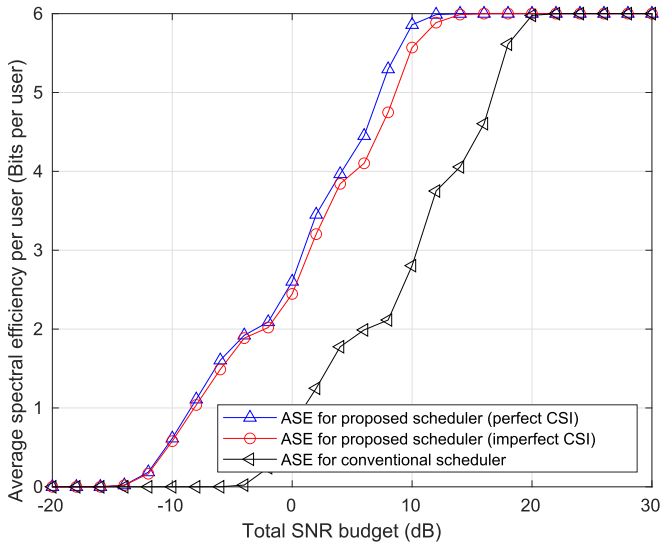

Fig. 8. Theoretical average spectral efficiencies of the maximum SNR and maximum rate scheduling policies in (32) and (33) and its simulation ones in $SER_T = 10^{-2}$ and Middleton class A noise environment with $(A, \Gamma) = (10^{-3}, 0.1)$. For simulation, $N_W = N_I = 10$.

Fig. 8 shows average spectral efficiency of the maximum SNR and the maximum rate scheduling schemes in $SER_T = 10^{-2}$ and impulsive noise parameters of $(A, \Gamma) = (10^{-3}, 0.1)$. As shown in Fig. 8, the average spectral efficiency of the maximum rate scheduling scheme is noticeably higher than that of the maximum SNR scheduling scheme, because the users in an impulsive noise environment adopt higher modulation orders, and thus transmit higher transmission rate, even in low SNR regime. Since the highest modulation order is 64-QAM in the simulations, the average spectral efficiency of the two scheduling schemes converges to six in high SNR regime. At SNR $= 5$ dB, the average spectral efficiency of the maximum rate scheduling scheme is higher than that of the maximum SNR scheduling by about 124%.

As can be seen in the figure, there is performance loss for the proposed scheduling scheme with imperfect CSI compared to the scheme with perfect CSI to a certain extent in high SNR region, but it is not significant because inaccurate estimations may lead to a bit lower spectrum utilization but occurs infrequently. It is worth mentioning that the proposed scheduling scheme always outperforms the conventional scheduling scheme significantly in terms of average spectral efficiency throughout the whole SNR region. In addition, even the proposed scheme with imperfect CSI provides far higher performance than the conventional scheduling with perfect

$$
\begin{aligned}
C^{(p)} &= \sum_{k=0}^{N_I-1} \binom{N_I-1}{k} \sum_{l=0}^{N_W-1} \binom{N_W-1}{l} (-1)^{k+l} (C_1 + C_2 - C_3) \\
&= \sum_{k=0}^{N_I-1} \binom{N_I-1}{k} \sum_{l=0}^{N_W-1} \binom{N_W-1}{l} (-1)^{k+l} \times \log_2(e) \Bigg(N_I \lambda_I \frac{E_1\big(((k+1)\lambda_I + l\lambda_W)\gamma_2^{(w)}\big)}{(k+1)\lambda_I + l\lambda_W} \\
&\quad + N_W \lambda_W \frac{E_1\big((k\lambda_I + (l+1)\lambda_W)\gamma_2^{(w)}\big)}{k\lambda_I + (l+1)\lambda_W} - (N_W\lambda_W + N_I\lambda_I) \frac{E_1\big(((k+1)\lambda_I + (l+1)\lambda_W)\gamma_2^{(w)}\big)}{(k+1)\lambda_I + (l+1)\lambda_W} \Bigg). \qquad (47)
\end{aligned}
$$

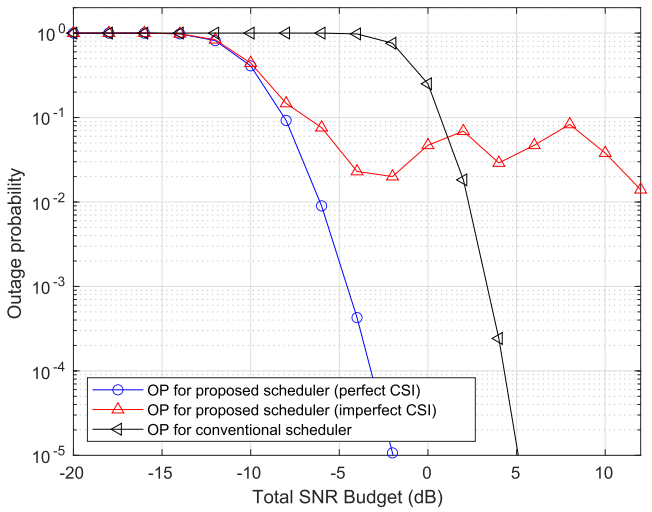

Fig. 9. Theoretical outage probabilities of systems with the maximum SNR and maximum rate scheduling policies in (35) and (36), and its simulation ones in $SER_T = 10^{-2}$ and Middleton class A noise environment with $(A, \Gamma) = (10^{-3}, 0.1)$. For simulation, $N_W = N_I = 10$.

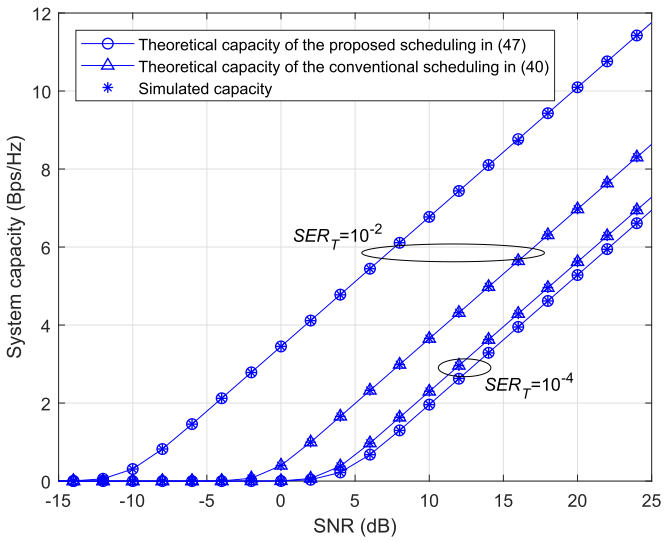

Fig. 10. Theoretical capacities of the maximum SNR and maximum rate scheduling policies in (40) and (47), and its simulation ones in $(A, \Gamma) = (10^{-3}, 0.1)$ and $SER_T = 10^{-2}$ and 10^{-4}. For simulation, $N_W = N_I = 10$.

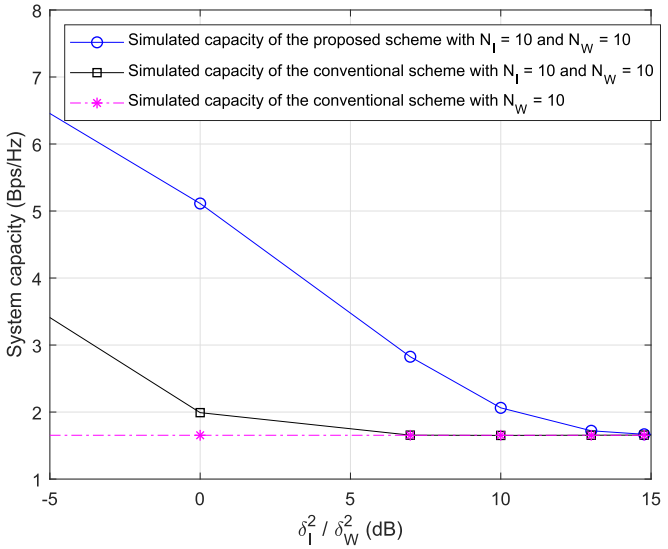

Fig. 11. Simulated capacities of the maximum SNR and maximum rate scheduling policies in $(A, \Gamma) = (10^{-3}, 0.1)$ and $SER_T = 10^{-2}$. For simulation, $N_W = N_I = 10$, where N_I is the number of users in impulsive noise, N_W is the number of users in AWGN.

CSI because the performance gain of the proposed scheme achieved by the right user selection based on the maximum rate is much larger than the performance loss caused by an estimation error. This gives us an insight that careful user selection is very important in a mixed noise environment.

Fig. 9 illustrates outage probabilities of the maximum SNR and the maximum rate scheduling schemes in $SER_T = 10^{-2}$ and impulsive noise parameters of $(A, \Gamma) = (10^{-3}, 0.1)$. As shown in the figure, the outage probability of the maximum rate scheduling scheme is significantly lower than that of the maximum SNR scheduling scheme. For instance, at SNR $= -6.73$ dB, the outage probability of the maximum rate scheduling scheme is lower than 10^{-2}, whereas the maximum SNR scheduling scheme can hardly transmit. From this result, it is clear that, when the users are in mixed AWGN and impulsive noise environment, the users in impulsive noise dominate the overall performance of the scheduling scheme. The figure also shows the outage probability of the proposed scheme with imperfect CSI, where an error floor occurs like those of most communication systems with channel estimation error. Interestingly, however, the outage performance of the proposed scheme with imperfect CSI is not monotonically decreasing to a constant floor but rather oscillates within a certain range, which can be understood by the adaptive modulation.

Fig. 10 presents capacity of the maximum SNR and the maximum rate scheduling schemes in (40) and (47), along with simulations, in impulsive noise with $(A, \Gamma) = (10^{-3}, 0.1)$. Two different target SERs, $SER_T = 10^{-2}$ and 10^{-4}, are considered. If $SER_T > A$, as shown in the figure, the system capacity of the maximum rate scheduling scheme is much higher than that of the maximum SNR scheduling in impulsive noise with $(A, \Gamma, SER_T) = (10^{-3}, 0.1, 10^{-2})$. This is easily understood by the fact that the SNR thresholds for adaptive modulation in impulsive noise are much lower than those for AWGN and therefore low SNR users in impulsive noise are allowed to use higher order modulations. So, if users have the same SNR, the scheduler tends to select a user with impulsive noise. On the other hand, if $SER_T < A$, the SNR thresholds for an impulsive noise environment are larger than those for AWGN environment. Thus, if users have the same SNR, the scheduler tends to select a user with AWGN.

Fig. 11 shows capacity of the maximum SNR and the maximum rate scheduling schemes, along with simulations, in impulsive noise with $(A, \Gamma) = (10^{-3}, 0.1)$. Target SER, $SER_T = 10^{-2}$, is considered. The average powers of Gaussian noise and impulsive noise are σ_W^2 and σ_I^2, respectively. Average SNR σ_s^2/σ_W^2 equals to 5 dB. In the case of low σ_I^2/σ_W^2, the simulated capacity of the maximum rate scheduling is higher than that of the maximum SNR scheduling because SNR thresholds for adaptive modulation

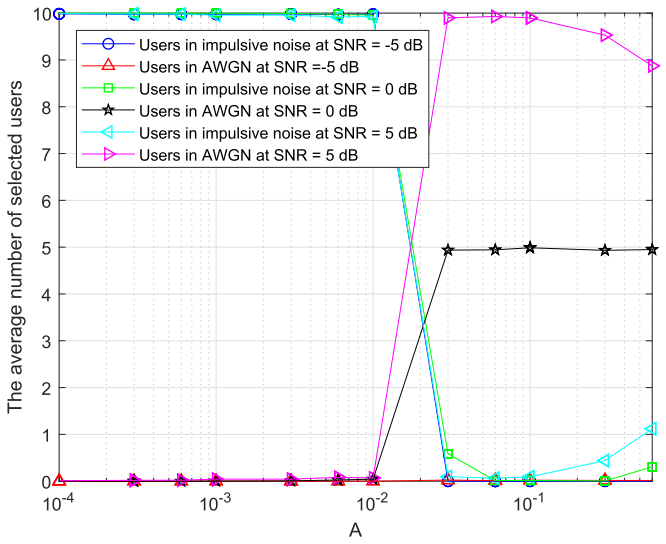

Fig. 12. The average number of users, selected by the maximum rate scheduling, in AWGN environment and impulsive noise environment with various A and $\Gamma = 0.1$. For simulation, $N_W = N_I = 10$ and $SER_T = 10^{-2}$.

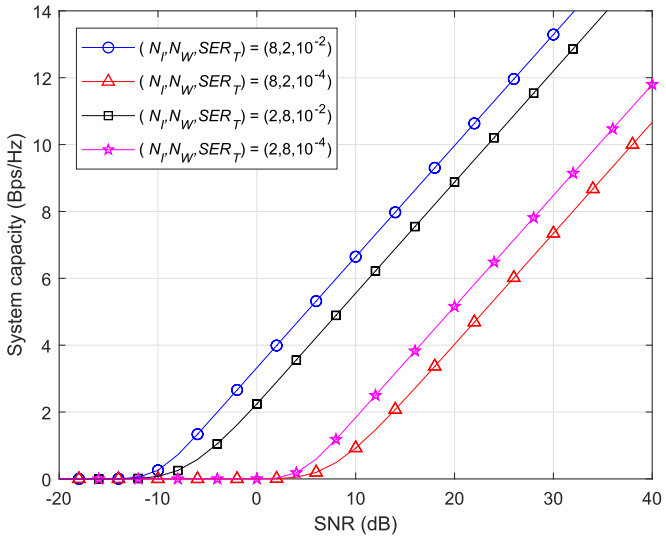

Fig. 13. System capacities with the maximum rate scheduling in $(A, \Gamma) = (10^{-3}, 0.1)$. For simulation, (N_I, N_W, SER_T) is set to (8,2,10^{-2}), (8,2,10^{-4}), (2,8,10^{-2}) and (2,8,10^{-4}).

in an impulsive noise environment is still lower than those for AWGN. In the case of high σ_I^2/σ_W^2, the simulated capacities of the maximum rate scheduling and the maximum SNR scheduling approaches to that of the maximum SNR scheduling with N_W because the scheduling policies select users in AWGN environment.

Fig. 12 illustrates the average number of users selected by the maximum rate scheduling scheme in AWGN environment and impulsive noise environment with $\Gamma = 0.1$ and various A. If $A \leq 10^{-2}$, the maximum rate scheduling scheme selects more users in impulsive noise than users in AWGN in low SNR region. However, in the case of $A > 10^{-2}$, more users in AWGN environment are selected as SNR increases, because the SNR threshold for BPSK in AWGN environment is lower than that in impulsive noise environment. Note that, with a high A, e.g. 0.3 and 0.6, more users in impulsive noise environment are likely to be selected because the SNR threshold for BPSK in an impulsive noise environment is reduced as A increases.

Fig. 13 compares system capacity of the maximum rate scheduling scheme with various number of users and target SERs, such as $(N_I, N_W, SER_T) = (8,2,10^{-2})$, $(8,2,10^{-4})$, $(2,8,10^{-2})$ and $(2,8,10^{-4})$, in impulsive noise with $(A, \Gamma) = (10^{-3}, 0.1)$. The scheduling scheme with $(N_I, N_W, SER_T) = (8,2,10^{-2})$ provides the highest system capacity because all the eight users in an impulsive noise environment are assigned higher order modulations even in low SNR region.

VIII. Conclusion

This article proposes the maximum rate scheduling scheme to maximize the system capacity in a multi-user environment where some users are under AWGN but others are exposed to impulsive noise. The conventional maximum SNR scheduling scheme cannot achieve the maximum capacity in such an environment because the conventional adaptive modulation is designed based on AWGN. Thus, this article first introduces approximate SER equations of various modulations in impulsive noise environment and defines an SNR ratio to compensate the SER loss by approximation. With the approximate SER, adaptive modulation in an impulsive noise environment is introduced along with a simple method of calculating the SNR thresholds, which is the most important parameter for adaptive modulation. In addition, average spectral efficiency, outage probability and capacity expressions for the maximum rate scheduling scheme are derived for performance evaluations. Simulation results show that system capacity and average spectral efficiency of the maximum rate scheduling scheme are respectively improved by 156% and 124% at SNR = 5 dB when ten users are in each environment compared to the performance of the conventional scheduling scheme in the scenario where all the twenty users in AWGN.

References

[1] D. Parruca and J. Gross, "Throughput analysis of proportional fair scheduling for sparse and ultra-dense interference-limited OFDMA/LTE networks," *IEEE Trans. Wireless Commun.*, vol. 15, no. 10, pp. 6857–6870, Oct. 2016.

[2] M.-R. Hojeij, C. Abdel Nour, J. Farah, and C. Douillard, "Waterfilling-based proportional fairness scheduler for downlink non-orthogonal multiple access," *IEEE Wireless Commun. Lett.*, vol. 6, no. 2, pp. 230–233, Apr. 2017.

[3] C. Cano, D. J. Leith, A. Garcia-Saavedra, and P. Serrano, "Fair coexistence of scheduled and random access wireless networks: Unlicensed LTE/WiFi," *IEEE/ACM Trans. Netw.*, vol. 25, no. 6, pp. 3267–3281, Dec. 2017.

[4] A. Rao and M.-S. Alouini, "Multiuser diversity with adaptive modulation in non-identically distributed nakagami fading environments," *IEEE Trans. Veh. Technol.*, vol. 61, no. 3, pp. 1439–1444, Mar. 2012.

[5] S. E. Sagkriotis, K. Kontovasilis, and A. D. Panagopoulos, "Proportional fair scheduling gains for AMC-aware systems under heterogeneous radio conditions," *IEEE Commun. Lett.*, vol. 16, no. 12, pp. 1984–1987, Dec. 2012.

[6] I.-H. Lee and S.-C. Kwon, "Performance analysis of quality-based channel state feedback scheme for wireless multicast systems with greedy scheduling," *IEEE Commun. Lett.*, vol. 19, no. 8, pp. 1430–1433, Aug. 2015.

[7] H. Li and X. Huang, "Multicast systems with fair scheduling in non-identically distributed fading channels," *IEEE Trans. Veh. Technol.*, vol. 66, no. 10, pp. 8835–8844, Oct. 2017.

[8] H. Oh and H. Nam, "Simple structure of a receiver for blind communication in impulsive noise," in *Proc. Int. Conf. Inf. Commun. Technol. Converg. (ICTC)*, Jeju, South Korea, Oct. 2016, pp. 588–592.
[9] J. Mitra and L. Lampe, "Design and analysis of robust detectors for TH IR-UWB systems with multiuser interference," *IEEE Trans. Commun.*, vol. 57, no. 8, pp. 2210–2214, Aug. 2009.
[10] P. Torio and M. G. Sanchez, "A study of the correlation between horizontal and vertical polarizations of impulsive noise in UHF," *IEEE Trans. Veh. Technol.*, vol. 56, no. 5, pp. 2844–2849, Sep. 2007.
[11] I. Landa, A. Blandzquez, M. Velez, and A. Arrinda, "Indoor measurements of IoT wireless systems interfered by impulsive noise from fluorescent lamps," in *Proc. IEEE Eur. Conf. Antennas Propag. (EUCAP)*, Paris, France, Mar. 2017, pp. 2080–2083.
[12] G. Bedicks, C. E. S. Dantas, F. Sukys, F. Yamada, L. T. M. Raunheitte, and C. Akamine, "Digital signal disturbed by impulsive noise," *IEEE Trans. Broadcast.*, vol. 51, no. 3, pp. 322–328, Sep. 2005.
[13] S. Niranjayan and N. C. Beaulieu, "Analysis of wireless communication systems in the presence of non-Gaussian impulsive noise and Gaussian noise," in *Proc. IEEE Wireless Commun. Netw. Conf. (WCNC)*, Sydney, NSW, Australia, Apr. 2010, pp. 1–6.
[14] Y. H. Ma, P. L. So, and E. Gunawan, "Performance analysis of OFDM systems for broadband power line communications under impulsive noise and multipath effects," *IEEE Trans. Power Del.*, vol. 20, no. 2, pp. 674–682, Apr. 2005.
[15] K. L. Blackard, T. S. Rappaport, and C. W. Bostian, "Measurements and models of radio frequency impulsive noise for indoor wireless communications," *IEEE J. Sel. Areas Commun.*, vol. 11, no. 7, pp. 991–1001, Sep. 1993.
[16] T. K. Blankenship, D. M. Kriztman, and T. S. Rappaport, "Measurements and simulation of radio frequency impulsive noise in hospitals and clinics," in *Proc. IEEE 47th Veh. Technol. Conf. Technol. Motion*, Phoenix, AZ, USA, May 1997, pp. 1942–1946.
[17] R. Prasad, A. Kegel, and A. de Vos, "Performance of microcellular mobile radio in a cochannel interference, natural, and man-made noise environment," *IEEE Trans. Veh. Technol.*, vol. 42, no. 1, pp. 33–40, Feb. 1993.
[18] S. Ambike, J. Ilow, and D. Hatzinakos, "Detection for binary transmission in a mixture of Gaussian noise and impulsive noise modeled as an alpha-stable process," *IEEE Signal Process. Lett.*, vol. 1, no. 3, pp. 55–57, Mar. 1994.
[19] L. Di Bert, P. Caldera, D. Schwingshackl, and A. M. Tonello, "On noise modeling for power line communications," in *Proc. IEEE Int. Symp. Power Line Commun. Appl. (ISPLC)*, Udine, Italy, Apr. 2011, pp. 238–288.
[20] J. Gadze, N. Pissinou, K. Makki, and G. Crosby, "On optimal slot allocation for reservation TDMA MAC protocol in shadow fading environment," in *Proc. Int. Symp. Wireless Commun. Syst. (ISWCS)*, Trondheim, Norway, Oct. 2007, pp. 809–813.
[21] Y. Cao, T. Jiang, M. He, and J. Zhang, "Device-to-device communications for energy management: A smart grid case," *IEEE J. Sel. Areas Commun.*, vol. 34, no. 1, pp. 190–201, Jan. 2016.
[22] M. Z. Win, P. C. Pinto, and L. A. Shepp, "A mathematical theory of network interference and its applications," *Proc. IEEE*, vol. 97, no. 2, pp. 205–230, Feb. 2009.
[23] K. Gulati, B. L. Evans, J. G. Andrews, and K. R. Tinsley, "Statistics of co-channel interference in a field of Poisson and Poisson-Poisson clustered interferers," *IEEE Trans. Signal Process.*, vol. 58, no. 12, pp. 6207–6222, Dec. 2010.
[24] E. Salbaroli and A. Zanella, "Interference analysis in a Poisson field of nodes of finite area," *IEEE Trans. Veh. Technol.*, vol. 58, no. 4, pp. 1776–1783, May 2009.
[25] K. Gulati, A. Chopra, B. L. Evans, and K. R. Tinsley, "Statistical modeling of co-channel interference," in *Proc. IEEE Globe Commun. Conf. (GLOBECOM)*, Honolulu, HI, USA, Nov. 2009, pp. 1–6.
[26] X. Yu, X. Dang, S.-H. Leung, Y. Liu, and X. Yin, "Unified analysis of multiuser scheduling for downlink MIMO systems with imperfect CSI," *IEEE Trans. Wireless Commun.*, vol. 13, no. 3, pp. 1344–1355, Mar. 2014.
[27] J. He, Z. Tang, Z. Tang, H.-H. Chen, and C. Ling, "Design and optimization of scheduling and non-orthogonal multiple access algorithms with imperfect channel state information," *IEEE Trans. Veh. Technol.*, vol. 67, no. 11, pp. 10800–10814, Nov. 2018.
[28] D. Middleton, "Statistical-physical models of electromagnetic interference," *IEEE Trans. Electromagn. Compat.*, vol. EMC-19, no. 3, pp. 106–127, Aug. 1977.
[29] L. Berry, "Understanding Middleton's canonical formula for class a noise," *IEEE Trans. Electromagn. Compat.*, vol. EMC-23, no. 4, pp. 337–344, Nov. 1981.
[30] S. Miyamoto, M. Katayama, and N. Morinaga, "Performance analysis of QAM systems under class a impulsive noise environment," *IEEE Trans. Electromagn. Compat.*, vol. 37, no. 2, pp. 260–267, May 1995.
[31] H. Oh and H. Nam, "Design and Performance Analysis of Non-linearity Preprocessors in an Impulsive Noise Environment," *IEEE Trans. Veh. Technol.*, vol. 66, no. 1, pp. 364–376, Jan. 2017.
[32] A. J. Goldsmith, *Wireless Communication*. Cambridge, U.K.: Cambridge Univ. Press, 2005.
[33] H. Oh and H. Nam, "Simple calculation of thresholds for adaptive modulation in middleton class a noise," in *Proc. IEEE Wireless Commun. Netw. Conf. (WCNC)*, San Francisco, CA, USA, Mar. 2017, pp. 1–6.
[34] H. Oh, H. Nam, and S. Park, "Adaptive threshold blanker in an impulsive noise environment," *IEEE Trans. Electromagn. Compat.*, vol. 56, no. 5, pp. 1045–1052, Oct. 2014.
[35] K. Vastola, "Threshold detection in narrow-band non-Gaussian noise," *IEEE Trans. Commun.*, vol. COM-32, no. 2, pp. 134–139, Feb. 1984.
[36] H. Nam, Y.-C. Ko, and M.-S. Alouini, "Performance analysis of joint switched diversity and adaptive modulation," *IEEE Trans. Wireless Commun.*, vol. 7, no. 10, pp. 3780–3790, Oct. 2008.
[37] M.-S. Alouini and A. J. Goldsmith, "Capacity of Rayleigh fading channels under different adaptive transmission and diversity-combining techniques," *IEEE Trans. Veh. Technol.*, vol. 48, no. 4, pp. 1165–1181, Jul. 1999.

Hyungkook Oh (Member, IEEE) received the B.S. and Ph.D. degrees from Hanyang University, in 2012 and 2018, respectively, all in electrical and communications engineering. His research interests include communication system design in an impulsive noise environment, signal processing for wireless communications, secure communications, and energy harvesting. He has received numerous scholarships, such as a Korean Government scholarship for undergraduate study and the M.S. and Ph.D. degrees scholarship.

Haewoon Nam (Senior Member, IEEE) received the B.S. degree from Hanyang University, Seoul, South Korea, the M.S. degree from Seoul National University, and the Ph.D. degree in electrical and computer engineering from The University of Texas at Austin, Austin, TX, USA. From 1999 to 2002, he was with Samsung Electronics, Suwon, South Korea, where he was engaged in the design and development of code division multiple access and global system for mobile communications (GSM)/general packet radio service baseband modem processors. In the summer of 2003, he was with the IBM Thomas J. Watson Research Center, Yorktown Heights, NY, USA, where he performed extensive radio channel measurements and analysis at 60 GHz. In the fall of 2005, he was with the Wireless Mobile System Group, Freescale Semiconductor, Austin, where he was engaged in the design and test of the worldwide interoperability for microwave access (WiMAX) medium access control layer. His industry experience also includes work with the Samsung Advanced Institute of Technology, Kiheung, South Korea, where he participated in the simulation of multi-input–multi-output systems for the Third-Generation Partnership Project (3GPP) Long-Term Evolution (LTE) standard. In October 2006, he joined the Mobile Devices Technology Office, Motorola, Inc., Austin, where he was involved in algorithm design and development for the 3GPP LTE mobile systems, including modeling of 3GPP LTE modem processor. Later in 2010, he was with Apple Inc., Cupertino, CA, USA, where he worked on research and development of next-generation smart mobile systems. Since March 2011, he has been with the Division of Electrical Engineering, Hanyang University, Ansan, South Korea, where he is currently a Professor. He received the Korean Government Overseas Scholarship for his doctoral studies in the field of electrical engineering.